ARID ZONE JOURNAL OF ENGINEERING, TECHNOLOGY & ENVIRONMENT
AZOJETE September 2025. Vol.21(3):702-716
Published by the Faculty of Engineering, University of Maiduguri, Maiduguri, Nigeria.
Print ISSN: 1596-2490, Electronic ISSN: 2545-5818
https://doi.org/10.63958/AZOJETE/2025/21/03/003
www.azojete.com.ng

ORIGINAL RESEARCH ARTICLE

EFFECT OF ADSORBENT DOSAGE ON THE KINETICS AND ISOTHERMS OF LEAD(II) REMOVAL FROM AQUEOUS SOLUTION USING CORN HUSK

A. A. Rasheed*, H. S. Muhammad, Y. Jakada, and N. Salahudeen

Department of Chemical and Petroleum Engineering, Faculty of Engineering, Bayero University Kano, PMB 3011, Kano, Nigeria.
**Corresponding author's email: aarasheed.cpe@buk.edu.ng*

ARTICLE INFORMATION

Received: 19th May 2025
Revised: 9th July 2025
Accepted: 12th July 2025

Keywords:
Adsorption
Dosage
Isotherms
Kinetics
Lead
Corn husk

ABSTRACT

Heavy metal contamination in water presents a critical environmental challenge, necessitating effective and sustainable solutions. This study explores the use of natural corn husk as an adsorbent for lead (II) removal from aqueous solutions. The corn husk was processed by drying, crushing, and sieving through a 75 µm mesh screen, followed by characterization using scanning electron microscopy (SEM), Fourier-transform infrared (FTIR) spectroscopy, and Brunauer-Emmett-Teller (BET) analysis. Batch adsorption experiments were conducted to investigate the effect of adsorbent dosage on the isotherms and kinetics of lead (II) removal. The results revealed that the percentage removal of lead increased with both adsorbent dosage and contact time, achieving equilibrium at 105 minutes. The highest removal efficiencies were 73%, 93%, and 96% for dosages of 0.5 g/L, 1 g/L, and 1.5 g/L, respectively. However, the adsorption capacity decreased with increasing dosage, from 111.72 mg/g to 49.06 mg/g. FTIR analysis confirmed the presence of functional groups such as hydroxyl, carboxyl, and ether groups, which contributed to the adsorption mechanism through chemisorption. Similarly, BET results showed a high surface area of 114.55 m^2/g with microporous characteristics, while SEM micrographs revealed a dense, rough, and porous morphology with well-distributed active sites. Furthermore, Isotherm analysis demonstrated that the Langmuir model provided the best fit across all dosages, indicating monolayer adsorption with maximum adsorption capacities (q_m) ranging from 85 mg/g to 178.57 mg/g. Separation factor (R_L) values of 0.2 and 0.19 at lower dosages indicated favorable adsorption conditions, while R_L = 0 at 1.5 g/L suggested irreversible adsorption. Kinetic studies confirmed the pseudo-second-order model as the most accurate across all dosages, highlighting chemisorption as the rate-determining mechanism. These findings underscore the significant role of adsorbent dosage in adsorption efficiency and provide insights into optimizing isotherms and kinetics for lead removal using corn husk.

1.0 Introduction

Heavy metal contamination, particularly lead, in water sources present a global challenge due to its profound health and environmental repercussions (Wang *et al.*, 2022). Lead, a non-biodegradable and highly toxic metal, infiltrates aquatic ecosystems primarily through industrial discharges such as those from battery manufacturing, mining operations, metal finishing processes, and electronic waste recycling (Adeogun *et al.*, 2010; Moyo *et al.*, 2013;). Even trace amounts of lead exposure pose significant risks, including neurological impairments, renal dysfunction, and developmental disorders, underscoring the critical need for its efficient removal from aqueous media (Kumar *et al.,* 2024; Zafar *et al.,* 2024). In recent years, biosorption has gained significant attention as a cost-effective and eco-friendly approach for removing heavy metals from contaminated environments (Khalid *et al.,* 2023; Reti *et al.,* 2024; Wang *et al.,* 2024). Notably, agricultural waste, due to its availability and low cost, has emerged as a promising adsorbent in biosorption processes (Moosa *et al.,* 2016; Ayari *et al.,* 2018).

Among agricultural byproducts, corn is one of the world's most widely cultivated crops and has emerged as a valuable resource for addressing environmental challenges through its conversion into adsorbents (Aguilar-Arteaga *et al*., 2022; Low *et al.,* 2022; Onyekwere *et al.,* 2024). Corn cultivation generates substantial amounts of agricultural residues, including corn husk, which are often discarded or underutilized. Corn husk, primarily composed of cellulose, hemicellulose, and lignin, is rich in functional groups such as hydroxyl and carboxyl, which facilitate the binding of metal ions (Moyo *et al*., 2013; Ratna *et al.,* 2022; Enawgaw *et al.,* 2023).

Given its physicochemical characteristics, corn husk is a promising material for the removal of lead from aqueous systems. Several studies (Guyo *et al*., 2015; Mireles *et al.,* 2019; Assirey and Altamimi, 2021; Chen *et al.,* 2022; Sawant *et al.,* 2022; Phaenark *et al.,* 2023) have reported its efficacy in lead biosorption, yet critical aspects of the adsorption mechanism remain underexplored In particular, the influence of adsorbent dosage on the kinetics and equilibrium behavior of lead biosorption has not been thoroughly investigated. Adsorbent dosage plays a fundamental role in determining the availability of binding sites and influences the dynamic interaction between adsorbent and adsorbate. At higher dosages, aggregation or saturation effects may alter surface properties, potentially affecting both adsorption capacity and model applicability (Ezeh *et al.,* 2017; Aniagor *et al.,* 2022; Amaibi *et al.,* 2024).

In this study, the focus is placed on evaluating how varying corn husk dosages affect the kinetic profiles and equilibrium isotherms of lead biosorption from aqueous solutions. The intention is to examine adsorption dynamics using both pseudo first order (PFO) and pseudo second order (PSO) kinetic models, alongside Langmuir and Freundlich isotherms, across a range of dosages. By systematically assessing these relationships, the study seeks to clarify the role of dosage in controlling biosorption behavior and improve understanding of how dosage-dependent mechanisms influence metal uptake processes.

2. Materials and Method

2.1 Materials and Analytical Equipment

The reagents and main apparatus utilized in this study include the following: analytical-grade lead chloride (Sigma-Aldrich, Germany), corn husk sourced from CDA (BUK), a crusher (220–240V Crusher, China), a scanning electron microscope (Phenom ProX, ThermoFisher Scientific, USA), and equipment for Brunauer-Emmett-Teller (BET) analysis (Nova 11.03A, USA). A Fourier transform infrared (FTIR) spectrophotometer (Spotlight 200i, PerkinElmer, USA), a 0.45 µm filter (Whatman, UK), and an atomic absorption spectrometer (AAS) (PinAAcle 900H, PerkinElmer, USA) were also employed.

Additional instruments included a pH meter (ST2100-B, Ohaus, USA), an orbital shaker (Joanlab OS-20, China), an oven (Genlab Ltd., England), a mesh sieve (Kelsons, India), and a weighing balance (Ohaus SP202, Scout Pro, USA). Distilled water used throughout the experiments was produced using a water distiller (SZ-96, Mon Scientific, Nigeria). Other essential items included a stopwatch and standard laboratory glassware.

2.2 Collection and Preparation of Adsorbent

Corn husk was sourced from the Centre for Dryland Agriculture (CDA) at Bayero University Kano. It was thoroughly washed with distilled water to remove dirt and impurities, followed by sun drying for two days. The husk was then further dried in an oven at 105°C for 24 hours. After drying, the husk was crushed, ground, and sieved to produce a fine powder with an average particle size of approximately 150 µm. These preparation conditions were adopted based on established protocols reported in the studies like Mukhlish *et al.* (2023), Said *et al.* (2024) and Erdem and Öner (2025). The resulting corn husk powder was stored in an airtight polyethylene bag at room temperature until it was needed for use.

2.3 Characterization of the cornhusk adsorbent

The physicochemical properties of the corn husk adsorbent were evaluated using standard analytical techniques. Scanning Electron Microscopy (SEM) coupled with Energy-Dispersive X-ray Spectroscopy (EDX) was employed to examine the surface morphology and elemental composition of the material, following the procedures outlined by Goldstein *et al.* (2017). The functional groups present on the adsorbent surface were identified through Fourier Transform Infrared Spectroscopy (FTIR) in the range of 4000–600 cm^{-1}, as described by Coates (2000). The specific surface area and pore size distribution were determined using Brunauer–Emmett–Teller (BET) analysis, with sample preparation and data interpretation performed in accordance with the guidelines provided by Sing *et al.* (1985).

Corresponding author's email address: aarasheed.cpe@buk.edu.ng

2.3 Biosorption Adsorption Studies

Batch adsorption studies were conducted following the methods outlined by Chen *et al. (*2022) and Batool *et al.* (2018). A synthetic solution containing 100 mg/L of lead (II) chloride was initially prepared using distilled water. The experiments were designed to vary one parameter at a time while maintaining others constant. Specifically, two process parameters namely contact time and adsorbent dosage, were tested at three levels, with pH, temperature, and agitation rate held constant as detailed in Table 1.

Table 1: Experimental Design for Removal of Lead from aqueous solution

Run	Dosage	Time	Frequency of sampling
1	0.5 g/L	120 mins	15 mins
2	1.0 g/L	120 mins	15 mins
3	1.5 g/L	120 mins	15 mins

For each experimental run, 80 mL of the synthetic solution was combined with a specified amount of the prepared adsorbent in a 120 mL bottle flask. Eight bottles were used per run, with one bottle sacrificed every 15 minutes to facilitate time resolved sampling, allowing for the measurement of concentration changes over the course of the experiment. The bottles were agitated on an orbital shaker at a constant speed of 175 rpm under room temperature conditions. At each designated sampling interval, the solution was filtered through a 0.45 µm filter paper, and the residual metal concentration in the supernatant was determined using an Atomic Absorption Spectrophotometer.

The percentage of metal ion removal and adsorption capacity of the adsorbent (metal uptake) was calculated using Equations 1 and 2 respectively.

$$Removal\ (\%) = \frac{(C_i - C_f)}{C_i} \times 100 \quad (1)$$

$$q_e = \frac{V(C_i - C_f)}{M} \quad (2)$$

Where C_i (mg/L) is the initial adsorbate concentration, C_f (mg/L) is the final adsorbate concentration, q_e (mg/g) is the amount of metal ion adsorbed per unit mass of adsorbent, V (L) is the solution's volume and M (g) is the amount of the adsorbent.

2.5 Determination of Biosorption Isotherms

The adsorption isotherm of lead in this study was analyzed using Langmuir and Freundlich models. The Langmuir and Freundlich models used are presented in equation (3) and (4) respectively (Sutirman *et al.,* 2018).

$$\frac{C_e}{q_e} = \frac{1}{K_L q_m} + \frac{C_e}{q_m} \quad (3)$$

$$log q_e = log K_F + \frac{1}{n} \log C_e \quad (4)$$

Where q_e is adsorption capacity at equilibrium (mg/g), q_m is the maximum capacity at equilibrium (mg/g), K_L is the Langmuir constant related to the affinity of the binding site (l/mg), Ce is the adsorbate equilibrium concentration (mg/L), K_F and 1/n are Freundlich constants related to adsorption capacity and affinity of the binding site respectively.

2.6 Determination of Biosorption Kinetics

The kinetics of the metals adsorption was studied using two models: pseudo first order (PFO) and pseudo second order (PSO) using equations (5) and (6) respectively (Zhang *et al.,* 2013).

$$\log(q_e - q_t) = \log q_e - \frac{k_1}{2.303} t \quad (5)$$

$$\frac{t}{q_t} = \frac{1}{k_2 q_e^2} + \frac{1}{q_e} t \quad (6)$$

Corresponding author's email address: aarasheed.cpe@buk.edu.ng

Where, q_e is adsorption capacity at equillibrium (mg/g), q_t (mg/g) is the adsorption capacity at any given time t (s), k_1 (s^{-1}) and k_2 (s^{-1}) are the rate constant of pseudo-first-order and pseudo-second-order respectively.

3. Results and Discussion

3.1 SEM Results

The SEM micrograph of corn husk in Plate 1 reveals a distinctively rough and fibrous surface morphology characterized by mountainous textures and irregular ridges. This can be attributed to its inherent lignocellulosic composition, primarily consisting of cellulose, hemicellulose, and lignin. This structural nature is consistent with the findings of Kambli *et al.* (2016), who noted that the limited presence of encrusting substances in corn husk fibers contributes to their distinctly rough and irregular surface texture. While no visible macropores were observed at the imaging scale, the material's heterogeneous and coarse surface suggests the possible presence of micropores, which are not easily detectable via conventional SEM. This rough texture significantly increases the external surface area and provides numerous micro-scale crevices and binding sites, enhancing the potential for lead ion attachment.

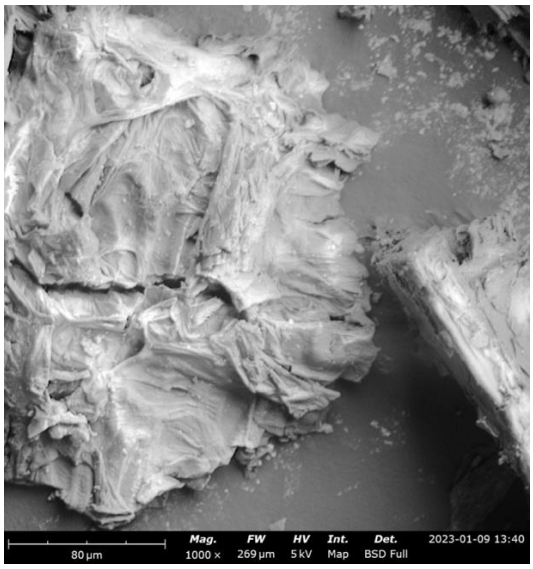

Plate 1: SEM of natural corn husk at 1000x magnification

The structural ruggedness and physical integrity of the corn husk further indicate a material capable of withstanding mechanical stress during adsorption processes. These features are critical in supporting both physical adsorption and chemisorption, driven by the availability of surface functional groups such as hydroxyl and carboxyl moieties. The surface topography, rather than visible porosity, appears to be the dominant contributor to its biosorptive behavior. This interpretation aligns with findings by Arunakumara *et al.* (2013) and Ponce *et al.* (2021), who similarly noted that surface roughness and the potential for microporosity play essential roles in the adsorption efficiency of lignocellulosic biosorbents. Therefore, the observed microstructural characteristics affirm the suitability of corn husk as a sustainable and effective biosorbent for lead removal from aqueous solutions.

The elemental composition determined through EDX analysis reveals the presence of C, O, K, P, Mg, Cl, Ca, and Si, as shown in Figure 1. The adsorbent in this study exhibits a carbon content of 50%, further confirming that corn husk is rich in lignite. This observation aligns with the findings of Reddygunta *et al.* (2023) and Ismail *et al.* (2022), who reported carbon contents of up to 47% and 55%, respectively, in corn husk. According to Danish *et al.* (2018), materials with carbon content ranging from 50% to 90% are classified as lignite-rich and are well-suited for activated carbon production. The carbon content observed in this study surpasses the values reported in other studies such as Kwaghger and Ibrahim (2013) and De Bouanzi *et al.* (2024), highlighting the superior composition of the corn husk used in this research. Additionally, the substantial surface oxygen atoms present in the corn husk adsorbent enhance their reactivity with adsorbed metal ions like lead, promoting a higher biosorption efficiency. This improved activity aligns with the Mars–van Krevelen (MvK) mechanism frequently associated with metal-oxides, as suggested by Dey *et al.* (2021).

Corresponding author's email address: aarasheed.cpe@buk.edu.ng

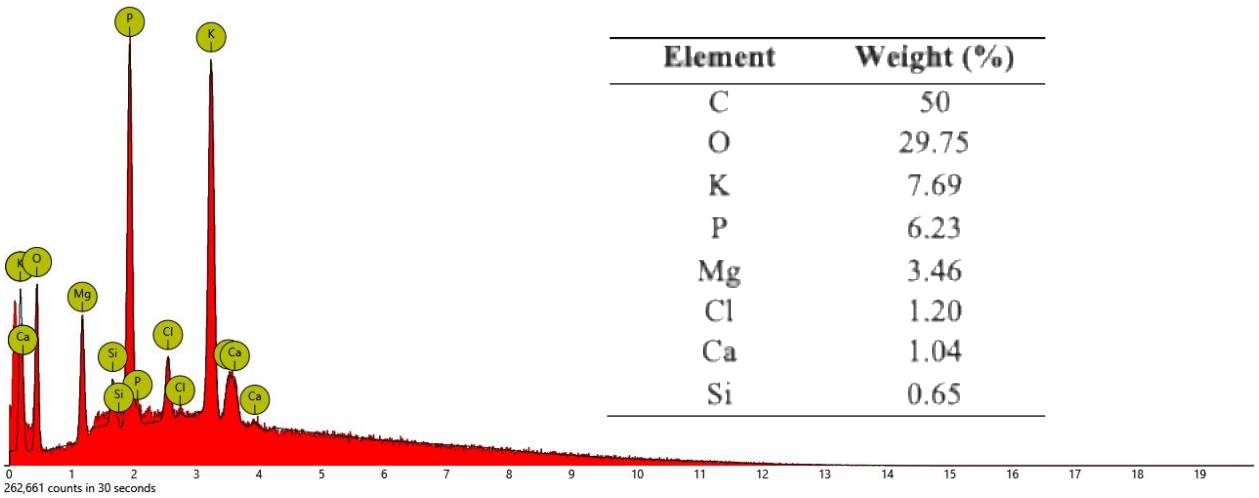

Element	Weight (%)
C	50
O	29.75
K	7.69
P	6.23
Mg	3.46
Cl	1.20
Ca	1.04
Si	0.65

Figure 1: EDX spectra of natural corn husk adsorbent

3.2 FTIR (Fourier Transform Infrared) Spectroscopy Analysis

The FTIR spectrum of corn husk in Figure 2 reveals an array of functional groups that are essential for its biosorption capabilities, highlighting its suitability as a natural adsorbent for heavy metal removal. The broad and intense peak at 3324.8 cm^{-1} corresponds to O-H stretching, a hallmark of hydroxyl groups that are abundant in the lignocellulosic components of corn husk, namely cellulose, hemicellulose, and lignin. These hydroxyl groups play a pivotal role in metal ion binding by forming hydrogen bonds and chelating with lead ions.

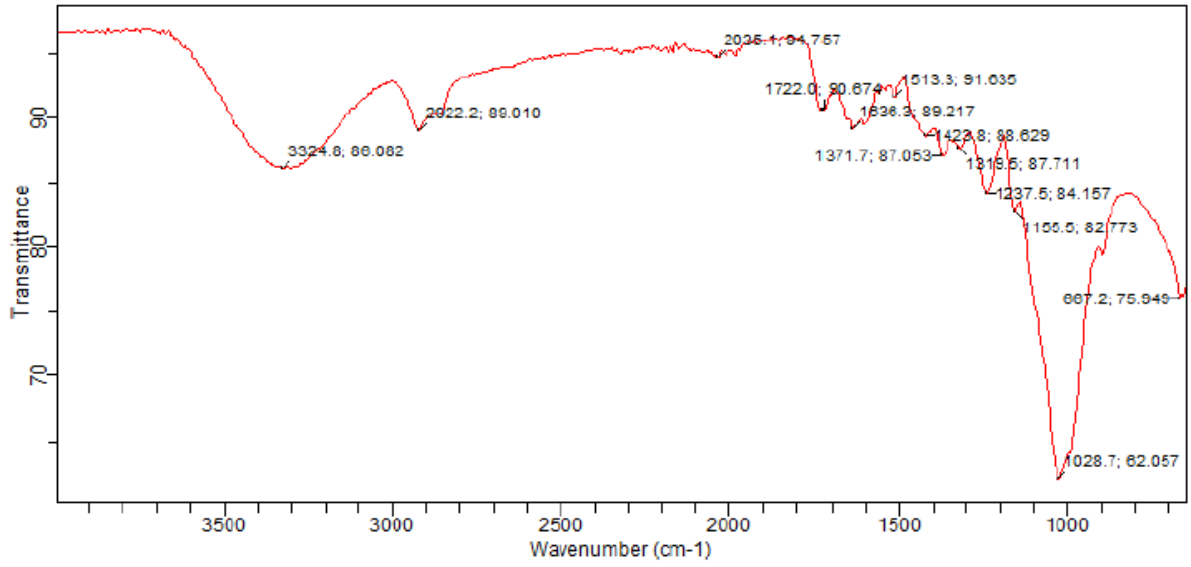

Figure 2. FTIR spectra of natural corn husk adsorbent.

The peak at 2822.2 cm^{-1} is attributed to C-H stretching vibrations, characteristic of aliphatic hydrocarbons or methylene groups, which indicate the presence of organic structural elements derived from lignin and other plant based compounds (Ray and Gupta, 2013; El-Araby *et al.,* 2017; Magoling and Macalalad, 2017; Chizoruo *et al.,* 2019)

A smaller peak at 2035.1 cm^{-1}, associated with C≡C or C≡N stretching, suggests the presence of alkynes or nitrile groups, possibly introduced during environmental exposure or chemical treatments. The pronounced peak at 1722.0 cm^{-1} corresponds to C=O stretching, representing carbonyl groups from carboxylic acids, esters, or ketones. These carbonyl groups are crucial in adsorption as they offer electron-rich sites for interaction with lead ions. At 1636.3 cm^{-1}, the spectrum shows C=C stretching or H-O-H bending, indicative of aromatic lignin structures or adsorbed water molecules, which contribute to the surface reactivity and

Corresponding author's email address: aarasheed.cpe@buk.edu.ng

facilitate ion exchange mechanisms. The peak at 1319.5 cm^{-1}, attributed to C-H or O-H bending, is associated with alcohols, phenols, or polysaccharides, further emphasizing the reactive nature of the corn husk. Meanwhile, the peaks at 1155.5 cm^{-1} and 1028.7 cm^{-1} correspond to C-O-C and C-O stretching vibrations, respectively, reflecting the presence of ether bonds and glycosidic linkages in cellulose and hemicellulose. These bonds provide structural integrity and additional binding sites for metal ions. The combination of these functional groups like hydroxyl, carbonyl, carboxyl, and ether creates a highly reactive surface on the corn husk, enriched with active sites for metal ion binding (Moosa *et al.,* 2016; Sun *et al.,* 2016; Dodevski *et al.,* 2017; El-Araby *et al.,* 2017; Lawal *et al.,* 2017; Assirey and Altamimi, 2021).

3.2 BET (Brunauer-Emmett-Teller) Analysis

The BET method was utilized to determine the surface area, pore volume, and pore size of the blended adsorbent, which are key parameters affecting its adsorption efficiency. Table 2 summarizes these properties for the corn husk adsorbent, which exhibited a BET surface area of 114.55 m^2/g. Although the majority of reported studies (Moosa *et al.,* 2016; Ayari *et al.,* 2018; Akram *et al.,* 2019; Bouzidi *et al.,* 2021; Tigori *et al.,* 2023) indicate that raw biosorbents, particularly those derived from lignocellulosic agricultural residues similar to the one used in this study, generally possess low Brunauer–Emmett–Teller (BET) surface areas typically below 30 m^2/g, the biosorbent in this work underwent a controlled oven-drying process at approximately 104 °C for 24 hours. While this treatment does not involve chemical or thermal activation in the conventional sense, it does constitute a form of mild thermal pre-treatment. Such drying may contribute to a modest increase in surface area as several previous studies have reported unexpectedly high surface areas exceeding 100 m^2/g for biosorbents that were not chemically activated, but rather subjected only to oven-drying or minimal processing. For example, recent studies have shown that certain unactivated agricultural biosorbents can exhibit high BET surface areas even without chemical or thermal activation. Specifically, sorghum husk and groundnut shell, when simply oven-dried and ground, have demonstrated BET surface areas of 139.5 m^2/g and 302.5 m^2/g, respectively, as reported by Hammari *et al.* (2022). These findings suggest that in certain cases, natural plant structure and internal porosity, when preserved and mildly altered through oven drying, may be sufficient to yield relatively high surface areas even in the absence of formal activation processes. The high surface area reported in this study provides a greater number of active sites, enhancing the interaction with contaminants such as heavy metals. This result underscores the effectiveness of the preparation method and the adsorbent's applicability for water treatment and heavy metal removal.

Table 2: BET results of natural corn husk adsorbent

Properties	Values
BET surface area (m^2/g)	114.5
BHJ pore volume (cm^3/g)	0.075
BHJ pore diameter (nm)	1.853

The pore volume and diameter of the adsorbent, measured using the Barrett, Joyner, and Halenda (BJH) method, were 0.075 cm^3/g and 1.853 nm, respectively. Pore size distribution analysis revealed that the adsorbent predominantly exhibited microporous characteristics. Micropores, typically less than 2 nm in diameter, significantly enhance adsorption capacity by providing many active sites and a high surface area for interaction at the molecular level (Centeno *et al.,* 2003). Given the molecular size of lead ions (0.175 nm), they can easily penetrate and diffuse within the microporous structure of the adsorbent. This compatibility facilitates close interaction between the lead ions and the active sites, enabling efficient mechanisms such as ion exchange, physical adsorption, and chemisorption. These findings affirm the suitability of the corn husk adsorbent for effective lead removal from contaminated water.

3.4 Biosorption Studies

3.4.1 Effect of Contact Time and Dosage on Lead removal

The effects of adsorbent dosage and contact time on the percentage removal and adsorption capacity of lead (Pb) using natural corn husk are illustrated in Figure 3. The data demonstrate a clear trend where the percentage removal of lead increases with both contact time and adsorbent dosage.

Corresponding author's email address: aarasheed.cpe@buk.edu.ng

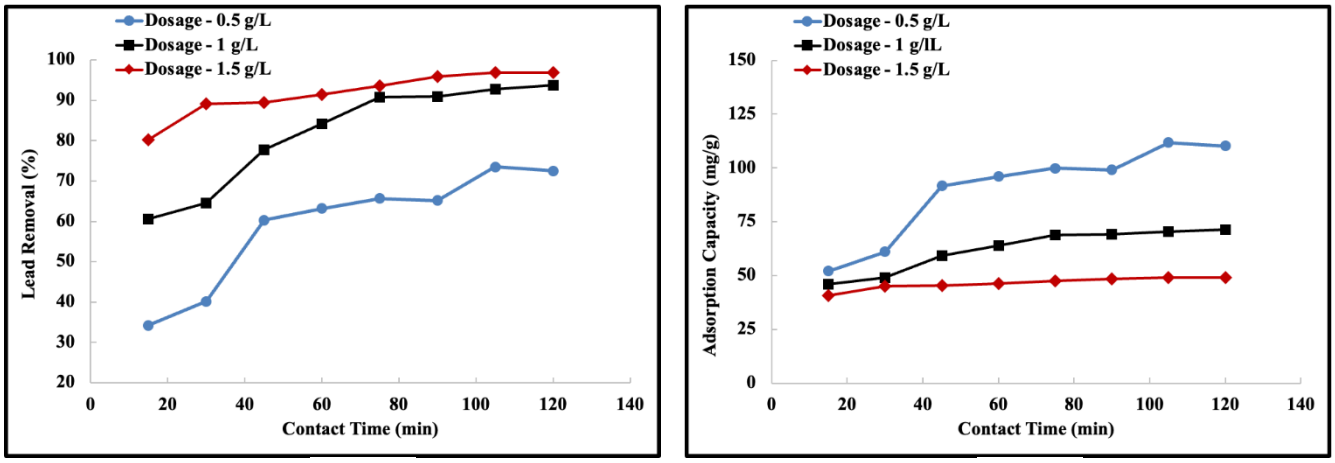

Figure 3: Effect of Dosage and Contact time on (a) lead removal and (b) adsorption capacity of corn husk adsorbent

Lead removal increased consistently and reached equilibrium within 105 minutes across all three runs with varying dosages. At a dosage of 0.5 g/L, the highest percentage removal was 73%. This efficiency improved significantly with increased dosages, reaching 93% at 1 g/L and 96% at 1.5 g/L. The figures also reveal that the adsorption process was rapid during the initial 60 minutes, attaining substantial removal rates before slowing down. This initial rapid phase can be attributed to the availability of ample external surface area on the adsorbent, facilitating fast adsorption kinetics. The slower phase that followed suggests the onset of internal diffusion as the rate-determining step, consistent with the findings of Li *et al.* (2008). This trend aligns with similar observations in prior studies (Rengaraj *et al.,* 2002; Mishra and Patel, 2009; Babalola *et al.,* 2016; Alghamdi *et al.,* 2019; Amaibi *et al.,* 2024).

The results further show an inverse relationship between adsorption capacity and adsorbent dosage. The adsorption capacity decreased from 111 mg/g at 0.5 g/L dosage to 49 mg/g at 1.5 g/L dosage. This phenomenon is supported by several studies (Shukla *et al.,* 2002; Li *et al.,* 2013; Babalola *et al.,* 2016; Ezeh *et al.,* 2017; Amaibi *et al.,* 2024), which suggest that increasing adsorbent dosage introduces more active sites, but the amount of lead ions adsorbed per unit mass of the adsorbent decreases. This reduction occurs as the ratio of available lead ions to the adsorbent mass decreases, leading to underutilization of the adsorbent's active sites. Additionally, higher dosages may result in overlapping or aggregation of adsorption sites, reducing the effective surface area and increasing diffusion path lengths (Ahluwalia and Goyal, 2007; Aniagor *et al.,* 2022). The aggregation of particles at higher dosages could also contribute to reduced surface area, as noted by Hashem *et al.* (2024).

At higher dosages, the introduction of more active sites does not proportionally enhance adsorption efficiency due to a reduction in the driving force of the concentration gradient, as explained by Jain *et al.* (2019). The splitting of the available adsorbate concentration among the excess active sites further diminishes the adsorption per gram of adsorbent. This decline is consistent with the fundamental adsorption equation (Equation 2), which relates the concentration gradient and adsorbent mass, showing the interplay between the numerator and denominator. These findings collectively highlight the importance of optimizing adsorbent dosage to balance percentage removal and adsorption capacity effectively.

3.4.2 Adsorption Isotherms

The effect of adsorbent dosage on adsorption isotherms provides critical insights into the adsorption behavior and efficiency of the corn husk adsorbent for lead removal. In this study, both the Langmuir and Freundlich isotherm models were analyzed across different adsorbent dosages (0.5 g/L, 1 g/L, and 1.5 g/L), revealing notable trends that illustrate how dosage impacts the adsorption process. The linearized forms of the Langmuir and Freundlich isotherms, derived using equations 3 and 4, are presented in Figure 4, with their corresponding correlation coefficients (R^2) and model parameters summarized in Table 3. Equilibrium isotherm parameters are essential for understanding the sorption mechanism, surface characteristics, and adsorption affinity of the adsorbent.

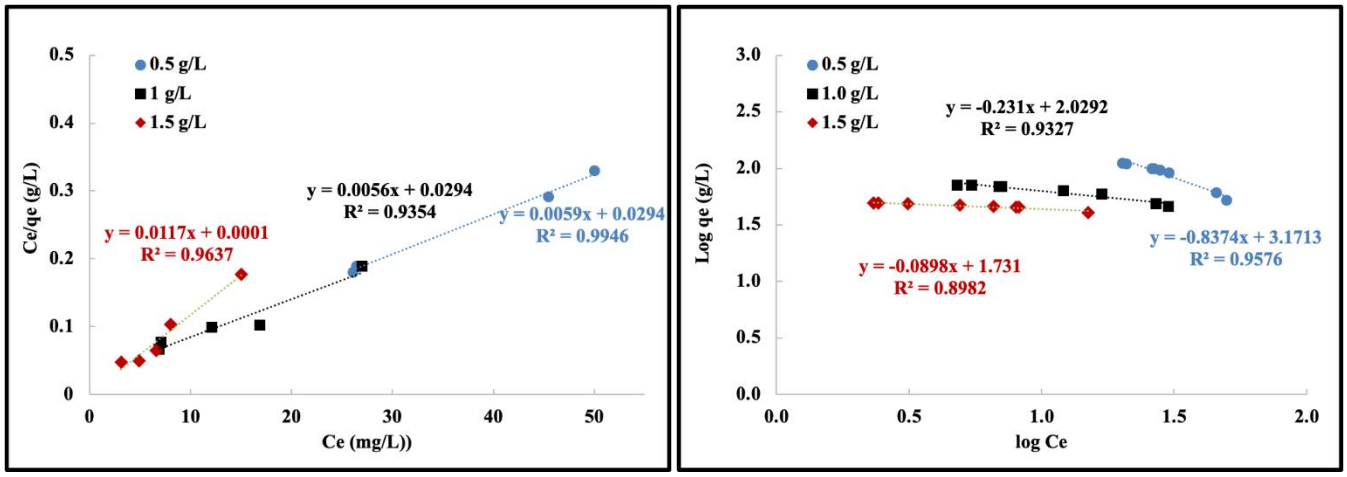

(a) (b)

Figure 4: Adsorption isotherms of (a) Langmuir (b) Freundlich models for lead removal on Corn husk

Table 3: model parameters for lead at different dosages using Langmuir and Freundlich models

Dosage (g/L)	Langmuir			Freundlich		
	R^2	K_L (L/mg)	R_L	R^2	n	K_f (L/g)
0.5	0.9946	0.20	0.06	0.9576	-1.19	1479.11
1	0.9354	0.19	0.07	0.9327	-4.33	107.15
1.5	0.9637	117	0	0.8982	-11.24	53.70

The Langmuir isotherm assumes adsorption occurs on a homogeneous surface through monolayer adsorption without interactions between adsorbed molecules. In contrast, the Freundlich isotherm describes non-ideal sorption on heterogeneous surfaces (Eze *et al.,* 2017; Amaibi *et al.,* 2024). The results in Table 3 show that the Langmuir isotherm exhibited higher correlation coefficients (R^2 = 0.99, 0.93, and 0.96 for 0.5 g/L, 1 g/L, and 1.5 g/L, respectively) than the Freundlich model (R^2 = 0.95, 0.93, and 0.85). Moreover, the Freundlich model showed negative values for the intensity parameter (***n***), suggesting a poor fit. These findings indicate that the Langmuir model better describes the adsorption process at all dosages studied, implying that the adsorption mechanism involves monolayer sorption on a homogeneous surface. The Langmuir isotherm also provided maximum monolayer adsorption capacities (q_m) of 169.49 mg/g, 178.57 mg/g, and 85 mg/g for dosages of 0.5 g/L, 1 g/L, and 1.5 g/L, respectively. This trend suggests that as the adsorbent dosage increases, the amount of lead ions adsorbed per unit mass of adsorbent decreases as already mentioned previously. The decrease in q_m and adsorption capacity with increasing dosage reflects a limitation in adsorption efficiency due to underutilization of active sites and possible aggregation of particles. For practical applications, it is essential to optimize the adsorbent dosage to achieve a balance between maximizing percentage removal and maintaining high adsorption capacity per unit mass.

The values obtained in this study are comparable to or exceed those reported for other agro-based adsorbents used for lead removal, such as those documented by Sekar *et al.* (2004), Imamoglu *et al.* (2008), Boudrahem *et al.* (2009), Martín-Lara *et al.* (2010), and Moyo *et al.* (2013). This highlights the corn husk's efficiency as an adsorbent.

The essential features of the Langmuir isotherm can be expressed in terms of a dimensionless constant separation factor (R_L)

$$R_L = \frac{1}{(1+(K_L C_i)} \quad 7$$

where C_i is the initial metal ion concentration in(mg/L) and K_L is the Langmuir equilibrium constant (L/mg). The separation factor derived from the Langmuir model, provides critical information about the nature of the adsorption process. Adsorption is considered irreversible when R_L= 0, favorable when (0 < R_L < 1), linear when R_L = 1 and unfavorable when R_L> 1 (Tseng *et al.*, 2010; Sun *et al.*, 2013). In this study, the R_L values for 0.5 g/L and 1 g/L dosages were 0.2 and 0.19, respectively, indicating favorable adsorption of lead on corn husk. However, at a higher dosage of 1.5 g/L, the R_L value was zero, signifying that the adsorption process was

Corresponding author's email address: aarasheed.cpe@buk.edu.ng

irreversible and overly strong. This indicates that at high dosages, the availability of an excessive number of active sites leads to near-complete binding of lead ions, with minimal reversibility aligning with the findings of Meroufel *et al.* (2013) and Balarak *et al.* (2017). These results further support the suitability of corn husk as an effective and sustainable biosorbent for heavy metal removal from aqueous solutions.

3.4.3 Adsorption Kinetics

Figure 5 presents the linearized plots of the PFO and PSO kinetic models for the adsorption of lead ions onto corn husk at varying adsorbent dosages. Model parameters and correlation coefficients (R^2) are summarized in Table 4 to aid interpretation.

The PSO model shows an excellent fit to the experimental data, with R^2 values of 0.96, 0.98, and 0.99 for adsorbent dosages of 0.5 g/L, 1.0 g/L, and 1.5 g/L, respectively. In contrast, the PFO model exhibits comparatively lower R^2 values of 0.87, 0.93, and 0.89, indicating that it does not adequately describe the adsorption kinetics under the studied conditions.

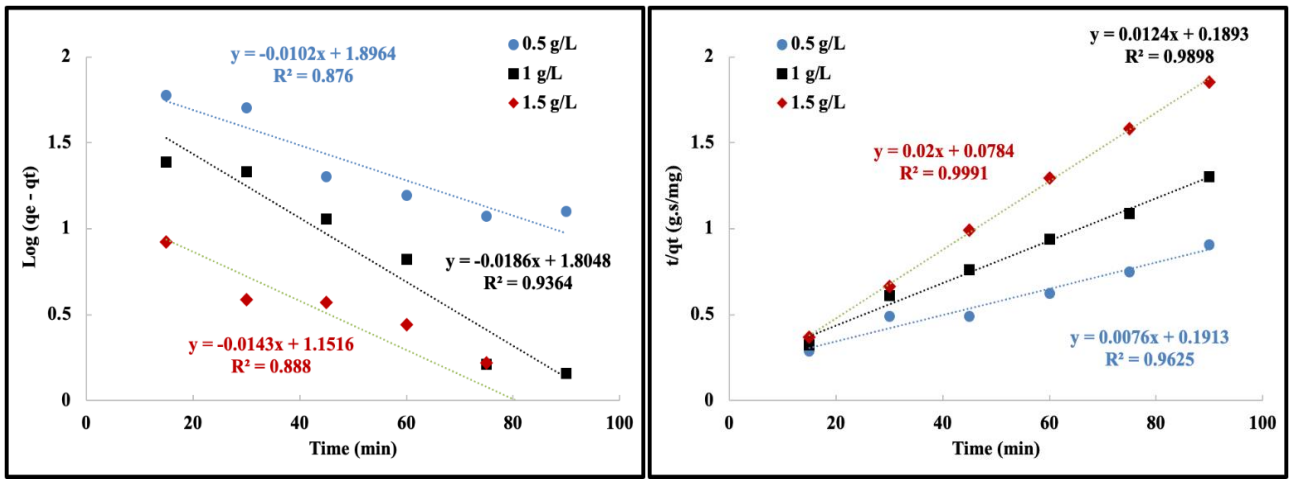

(a) **(b)**

Figure 5: Adsorption kinetic models (a) PFO (b) PSO models for lead removal on Corn husk

Table 4: Correlation coefficient and other model parameters for lead removal at different dosages using Pseudo-first order and Pseudo-second order models

Dosage (g/L)	Pseudo-first order			Pseudo-second order		
	R^2	k_1 (min^{-1})	qe (mg/g)	R^2	k_2 (g/mg min^{-1})	q_e (mg/g)
0.5	0.876	0.023	78.7	0.9625	0.0003	131.6
1	0.9364	0.043	63.1	0.9898	0.0008	80.6
1.5	0.888	0.033	14.2	0.9991	0.0051	50.0

Importantly from Figure 5, the adsorption capacities predicted by the PSO model were observed to decrease with increasing adsorbent dosage. The adsorption capacities predicted by the PSO model (q_e) were 131.57 mg/g, 80.65 mg/g, and 50 mg/g for 0.5 g/L, 1 g/L, and 1.5 g/L dosages, respectively. These values closely match the experimental equilibrium adsorption capacities (q_e) of 111.72 mg/g, 70.56 mg/g, and 49.06 mg/g, further validating the applicability of the PSO model. On the other hand, the adsorption capacities predicted by the PFO model (78.79 mg/g, 63.09 mg/g, and 14.2 mg/g) deviate significantly from the experimental values, confirming its inadequacy in describing the adsorption process.

The dominance of the PSO model indicates that the adsorption of lead onto corn husk is likely governed by chemisorption, which involves electron sharing or exchange between lead ions and the active functional groups on the adsorbent surface. This chemisorption mechanism is supported by FTIR analysis, which revealed the presence of functional groups such as hydroxyl, carboxyl, and ether groups, known for their high affinity for heavy metal ions. Chemisorption implies that the process is not solely surface-dependent but also involves strong, irreversible interactions between the adsorbate and the adsorbent. This observation aligns with previous findings by Badmus *et al.* (2007), Adeogun *et al.* (2010), Das and Mondal (2011), Robati (2013), Tan *et al.* (2020), and Revellame *et al.* (2020).

The findings of this study underscore the importance of optimizing adsorbent dosage for effective lead removal and highlight the potential of corn husk as a sustainable, efficient adsorbent for heavy metal remediation. The applicability of the PSO model provides a robust scientific foundation for employing agricultural waste-derived adsorbents in environmental cleanup efforts, consistent with the studies by Çelebi and Gok (2017) and Futalan *et al.* (2019). The effect of dosage on kinetics highlights the interplay between adsorption rate and capacity: at low dosage where the adsorption process is highly efficient, with a higher proportion of active sites utilized due to the high concentration gradient; and at high dosage where although the overall percentage removal increases due to the greater number of active sites, the adsorption capacity per unit mass decreases, and the kinetics slow down due to reduced driving force and site accessibility.

4. Conclusion

In conclusion, this study highlights the potential of using corn husk as an effective adsorbent for lead (II) removal from aqueous solutions, emphasizing the role of adsorbent dosage and contact time. The results demonstrated percentage removal of lead increased with higher dosages and longer contact times, achieving up to 96% removal at 1.5 g/L dosage and 105 minutes. Adsorption capacity decreased with increasing dosage, from 111.72 mg/g at 0.5 g/L to 49.06 mg/g at 1.5 g/L, due to underutilization of active sites and particle aggregation. However, adsorption capacity decreased with increasing dosage, attributed to underutilization of active sites and particle aggregation. Characterization using FTIR, SEM, and BET confirmed the presence of functional groups such as hydroxyl, carboxyl, and ether, a high surface area of 114.55 m^2/g, and a microporous, rough, and porous morphology, all contributing to the chemisorption mechanism. The Langmuir isotherm model provided the best fit, indicating monolayer adsorption with maximum adsorption capacities ranging from 85 mg/g to 178.57 mg/g. The separation factor (R_L) values of 0.2 and 0.19 at lower dosages indicated favorable adsorption conditions, whereas an R_L value of 0 at 1.5 g/L reflected irreversible adsorption behavior. Kinetic studies validated the pseudo-second-order model, highlighting chemisorption as the rate-determining step. While higher dosages improve overall removal efficiency, they reduce adsorption capacity per unit mass and may lead to irreversible adsorption at extreme dosages.

Acknowledgements

The authors are grateful to the Tertiary Education Trust Fund (TETFund), Abuja, for funding this project through their Institutional Base Research (IBR) grant No.: BUK/DRIP/TETF/0012

References

Adeogun, AI., Bello, OS. and Adeboye, MD. 2010. Biosorption of Lead Ions on Biosorbent Prepared from Plumb Shells (Spondias mombin): Kinetics and Equilibrium Studies: Biosorbent Prepared from Spondias mombin. Biological Sciences, 53(5): 246-251.

Aguilar-Arteaga, K., Castañeda-Ovando, A., Castañeda-Ovando, EP., Lira, BP. and Batalla, LD. 2024. Removal of heavy metal ions with magnetic carbon prepared from corncob biomass. Environmental Technology, 45(10): 1956–1968.

Ahluwalia, SS., and Goyal, D. 2007. Microbial and plant derived biomass for removal of heavy metals from wastewater. Bioresource technology, 98(12): 2243-2257.

Akram, M., Khan, B., Imran, M., Ahmad, I., Ajaz, H., Tahir, M., and Samad, SN. 2019. Biosorption of lead by cotton shells powder: characterization and equilibrium modeling study. International journal of phytoremediation, 21(2): 138-144.

Alghamdi, AA., Al-Odayni, AB., Saeed, WS., Al-Kahtani, A., Alharthi, FA., and Aouak, T. 2019. Efficient adsorption of lead (II) from aqueous phase solutions using polypyrrole-based activated carbon. Materials, 12(12): 2020.

Amaibi, PM., Egong, JF., Iwe, CR., and Obunwo, CC. 2024. Adsorption and Kinetic Studies for Removal of Fluoride in Aqueous System by Activated Carbon Produced from Lemon Peels. Journal of Applied Sciences and Environmental Management, 28(5): 1413-1419.

Aniagor, CO., Abdulgalil, AG., Safri, A., Elhmmali, MM., and Hashem, A. 2022. Preparation of amidoxime modified biomass and subsequent investigation of their lead ion adsorption properties. Cleaner Chemical Engineering, 2: 100013.

Corresponding author's email address: aarasheed.cpe@buk.edu.ng

Arunakumara, KIU., Walpola, BC., and Yoon, MH. 2013. Banana peel: A green solution for metal removal from contaminated waters. Korean Journal of Environmental Agriculture, 32(2): 108-116.

Assirey, EA., and Altamimi, LR. 2021. Chemical analysis of corn cob-based biochar and its role as water decontaminants. Journal of Taibah University for Science, 15(1): 111-121.

Ayari, F., Mezghuich, S., Othmen, AB., and Trabelsi-Ayadi, M. 2018. Evaluation of adsorptive capacity of natural biosorbent for dye removal as a contribution to environmental protection: effect of various parameters. Desalination and Water Treatment, 105: 332-342.

Babalola, JO., Omorogie, MO., Babarinde, AA., Unuabonah, EI., and Oninla, VO. 2016. Optimization Of The Biosorption Of Cr 3+, Cd 2+ And Pb 2+ Using A New Biowaste: Zea mays SEED CHAFF. Environmental Engineering & Management Journal (EEMJ), 15(7).

Badmus, MOA., Audu, TOK., and Anyata, B. 2007. Removal of copper from industrial wastewaters by activated carbon prepared from periwinkle shells. Korean Journal of Chemical Engineering, 24: 246-252.

Balarak, D., Mostafapour, F., Azarpira, H., and Joghataei, A. 2017. Langmuir, Freundlich, Temkin and Dubinin–radushkevich isotherms studies of equilibrium sorption of ampicilin unto montmorillonite nanoparticles. Journal of Pharmaceutical Research International, 20(2): 1-9.

Batool, F., Akbar, J., Iqbal, S., Noreen, S., and Bukhari, SNA. 2018. Study of isothermal, kinetic, and thermodynamic parameters for adsorption of cadmium: an overview of linear and nonlinear approach and error analysis. Bioinorganic chemistry and applications, 1: 3463724.

Boudrahem, F., Aissani-Benissad, F., and Aït-Amar, H. 2009. Batch sorption dynamics and equilibrium for the removal of lead ions from aqueous phase using activated carbon developed from coffee residue activated with zinc chloride. Journal of environmental management, 90(10): 3031-3039.

Bouzidi, A., Djedid, M., Ad, C., Benalia, M., Hafez, B., and Elmsellem, H. 2021. Biosorption of Co (II) ions from aqueous solutions using selected local Luffa Cylindrica: Adsorption and characterization studies. Moroccan Journal of Chemistry, 9(1).

Çelebi, H., and Gök, O. 2017. Evaluation of lead adsorption kinetics and isotherms from aqueous solution using natural walnut shell. International Journal of Environmental Research, 11: 83-90.

Centeno, TA., Marbán, G., and Fuertes, AB. 2003. Importance of micropore size distribution on adsorption at low adsorbate concentrations. Carbon, 41(4): 843-846.

Chen, F., Sun, Y., Liang, C., Yang, T., Mi, S., Dai, Y., and Yao, Q. 2022. Adsorption characteristics and mechanisms of Cd2+ from aqueous solution by biochar derived from corn stover. Scientific Reports, 12(1): 17714.

Chizoruo, IF., Onyekachi, IB., and Ebere, EC. 2019. Trace metal, FTIR and phytochemical analysis of Viscum album leaves harvested from Pentaclethra macrophylla. World News of Natural Sciences, 25: 61-71.

Coates, J. 2000. Interpretation of Infrared Spectra, A Practical Approach. In RA. Meyers (Ed.), Encyclopedia of Analytical Chemistry, Chichester: John Wiley & Sons Ltd: 10815–10837

Danish, M., and Ahmad, T. 2018. A review on utilization of wood biomass as a sustainable precursor for activated carbon production and application. Renewable and Sustainable Energy Reviews, 87: 1-21.

Das, B., and Mondal, NK. 2011. Calcareous Soil as a New Adsorbent to Remove Lead from Aqueous Solution: Equilibrium, Kinetic and Thermodynamic Study. Universal Journal of Environmental Research & Technology, 1(4).

De Bouanzi, MGG., Atheba, PG., Gbamé, SK., Aka, MA., and Trokourey, A. 2024. Preparation and Characterisation of Corncob-Based Biosorbents in Côte d'Ivoire. Advances in Materials Physics and Chemistry, 14(8): 178-195.

Dey, S., Basha, SR., Babu, GV., and Nagendra, T. 2021. Characteristic and biosorption capacities of orange peels biosorbents for removal of ammonia and nitrate from contaminated water. Cleaner Materials, 1: 100001.

Corresponding author's email address: aarasheed.cpe@buk.edu.ng

Dodevski, V., Janković, B., Stojmenović, M., Krstić, S., Popović, J., Pagnacco, MC., Popović , M. and Pašalić, S. 2017. Plane tree seed biomass used for preparation of activated carbons (AC) derived from pyrolysis. Modeling the activation process. Colloids and Surfaces A: Physicochemical and Engineering Aspects, 522: 83-96.

El-Araby, HA., Ibrahim, AMM., Mangood, AH., and Adel, AH. 2017. Sesame husk as adsorbent for copper (II) ions removal from aqueous solution. Journal of Geoscience and Environment Protection, 5(07).

Enawgaw, H., Tesfaye, T., Yilma, KT., and Limeneh, DY. 2023. Multiple Utilization Ways of Corn By-Products for Biomaterial Production with Bio-Refinery Concept; a Review. Materials Circular Economy, 5(1): 7.

Erdem, M., and Öner, A. 2025. Preparation and Characterization of Low-Cost Bio-Sorbent and a Novel Activated Carbon from Agro-Wastes for Efficient Cr (VI) Removal. Water, Air, & Soil Pollution, 236(5): 291.

Ezeh, K., Ogbu, I., Akpomie, K., Ojukwu, N., and Ibe, J. 2017. Utilizing the sorption capacity of local Nigerian sawdust for attenuation of heavy metals from solution: isotherm, kinetic, and thermodynamic investigations. Pacific Journal of Science and Technology, 18: 251-264.

Futalan, CM., Kim, J., & Yee, JJ. 2019. Adsorptive treatment via simultaneous removal of copper, lead and zinc from soil washing wastewater using spent coffee grounds. Water Science and Technology, 79(6): 1029-1041.

Goldstein, JI., Newbury, DE., Joy, DC., Lyman, CE., Echlin, P., Lifshin, E., Sawyer, L., and Michael, JR. 2017. Scanning Electron Microscopy and X-ray Microanalysis (4th ed.). Springer.

Guyo, U., Mhonyera, J., and Moyo, M. 2015. Pb (II) adsorption from aqueous solutions by raw and treated biomass of maize stover–a comparative study. Process Safety and Environmental Protection, 93: 192-200.

Hammari, AM., Misau, MI., Aroke, UO., Hamza, UD. and Yusuf, AA. 2021. Adsorption equilibrium and kinetics studies of congo red dye using groundnut shell and sorghum husk biosorbent. Journal of Biochemistry, Microbiology and Biotechnology, 9(1):.29-36.

Hashem, A., Aniagor, CO., Farag, S., Fikry, M., Aly, AA., and Amr, A. 2024. Evaluation of the adsorption capacity of surfactant-modified biomass in an aqueous acid blue 193 system. Waste Management Bulletin, 2(1): 172-183.

Imamoglu, M., and Tekir, O. 2008. Removal of copper (II) and lead (II) ions from aqueous solutions by adsorption on activated carbon from a new precursor hazelnut husks. Desalination, 228(1-3): 108-113.

Ismail, MS., Yahya, MD., Auta, M. and Obayomi, KS. 2022. Facile preparation of amine-functionalized corn husk derived activated carbon for effective removal of selected heavy metals from battery recycling wastewater. Heliyon, 8(5).

Jain, SN., Shaikh, Z., Mane, VS., Vishnoi, S., Mawal, VN., Patel, OR., and Gaikwad, MS. 2019. Nonlinear regression approach for acid dye remediation using activated adsorbent: Kinetic, isotherm, thermodynamic and reusability studies. Microchemical Journal, 148: 605-615.

Kambli, N., Basak, S., Samanta, KK. and Deshmukh, RR. 2016. Extraction of natural cellulosic fibers from cornhusk and its physico-chemical properties. Fibers and Polymers, 17: 687-694.

Khalid, M., Khan, N. A., Rahim, A., Shah, A., and Rahim, M. A. (2023). Efficacious sorption capacities for Pb(II) from contaminated water: A comparative study using biowaste and its activated carbon. ACS Omega, 8(17): 15141–15151.

Kumar, D., Mohan, MR., Krishnaiah, CV., Prasad, GLN., Sreedevi, B., and Naik, R. 2024. Toxicological Effects Of Lead On Human Health: A Comprehensive Review. Journal of Experimental Zoology India, 27(2).

Kwaghger, A., and Ibrahim, JS. 2013. Optimization of conditions for the preparation of activated carbon from mango nuts using HCl. American Journal of Engineering Research, 2(7): 74-85.

Lawal, IA., Chetty, D., Akpotu, SO., & Moodley, B. 2017. Sorption of Congo red and reactive blue on biomass and activated carbon derived from biomass modified by ionic liquid. Environmental nanotechnology, monitoring & management, 8: 83-91.

Li, TT., Liu, YG., Peng, QQ., Hu, XJ., Liao, T., Wang, H., and Lu, M. 2013. Removal of lead (II) from aqueous solution with ethylenediamine-modified yeast biomass coated with magnetic chitosan microparticles: Kinetic and equilibrium modeling. Chemical Engineering Journal, 214: 189-197.

Li, W., Zhang, L., Peng, J., Li, N., Zhang, S., and Guo, S. 2008. Tobacco stems as a low cost adsorbent for the removal of Pb (II) from wastewater: Equilibrium and kinetic studies. Industrial crops and products, 28(3): 294-302.

Low, WP., Lee, EY., Chang, FL., and Rahman, NA. 2022. Removal of heavy metals ions from aqueous solution using different pretreatment techniques of corn cob. Journal of Innovation and Technology, 290.

Magoling, BJA., and Macalalad, AA. 2017. Optimization and response surface modelling of activated carbon production from Mahogany fruit husk for removal of chromium (VI) from aqueous solution. BioResources, 12(2): 3001-3016.

Malik, R., Ramteke, DS., and Wate, SR. 2007. Adsorption of malachite green on groundnut shell waste based powdered activated carbon. Waste Management, 27(9): 1129–1138.

Martín-Lara, MÁ., Rico, ILR., Vicente, IDA., García, GB., and de Hoces, MC. 2010. Modification of the sorptive characteristics of sugarcane bagasse for removing lead from aqueous solutions. Desalination, 256(1-3): 58-63.

Meena, AK., Kadirvelu, K., Mishra, GK., Rajagopal, C., and Nagar, PN. 2008. Adsorptive removal of heavy metals from aqueous solution by treated sawdust (Acacia arabica). Journal of hazardous materials, 150(3): 604-611.

Meroufel, B., Benali, O., Benyahia, M., Benmoussa, Y., and Zenasni, MA. 2013. Adsorptive removal of anionic dye from aqueous solutions by Algerian kaolin: Characteristics, isotherm, kinetic and thermodynamic studies. J. Mater. Environ. Sci, 4(3): 482-491.

Mireles, S., Parsons, J., Trad, T., Cheng, C. L., and Kang, J. 2019. Lead removal from aqueous solutions using biochars derived from corn stover, orange peel, and pistachio shell. International Journal of Environmental Science and Technology, 16: 5817-5826.

Mishra, PC., and Patel, RK. 2009. Removal of lead and zinc ions from water by low cost adsorbents. Journal of hazardous materials, 168(1): 319-325.

Moosa, AA., Ridha, AM., and Hussien, NA. 2016. Adsorptive removal of lead ions from aqueous solution using biosorbent and carbon nanotubes. American Journal of Materials Science, 6(5): 115-124.

Moyo, M., Chikazaza, L., Nyamunda, BC., and Guyo, U. 2013. Adsorption batch studies on the removal of Pb (II) using maize tassel based activated carbon. Journal of Chemistry, 1: 508934.

Mukhlish, MZB., Nazibunnesa, S., Islam, S., Al Mahmood, AS., and Uddin, MT. 2023. Preparation of chemically and thermally modified water caltrop epicarp (Trapa natans L.) adsorbent for enhanced adsorption of Ni (II) from aqueous solution. Heliyon, 9(11).

Onyekwere, OS., Hambali, HU., Macaulay, FE., Haruna, AD., Ayinla, L., Ogundokun, PB., Sulyman, IA., Oyelade-Akinsola, OP. and Hayes, AI .2024. Modified corn cob adsorbent for heavy metal removal from wastewater. Savannah Journal of Science and Engineering Technology, 2(2): 033–040

Phaenark, C., Jantrasakul, T., Paejaroen, P., Chunchob, S., and Sawangproh, W. 2023. Sugarcane bagasse and corn stalk biomass as a potential sorbent for the removal of Pb (II) and Cd (II) from aqueous solutions. Trends in Sciences, 20(2): 6221-6221.

Ponce, J., da Silva Andrade, JG., dos Santos, LN., Bulla, MK., Barros, BCB., Favaro, SL., Hioka, N., Caetano, W. and Batistela, VR. 2021.. Alkali pretreated sugarcane bagasse, rice husk and corn husk wastes as lignocellulosic biosorbents for dyes. Carbohydrate Polymer Technologies and Applications, 2: 100061.

Ratna, AS., Ghosh, A., and Mukhopadhyay, S. 2022. Advances and prospects of corn husk as a sustainable material in composites and other technical applications. Journal of cleaner production, 371: 133563.

Corresponding author's email address: aarasheed.cpe@buk.edu.ng

Ray, A., and Gupta, SD. 2013. A panoptic study of antioxidant potential of foliar gel at different harvesting regimens of Aloe vera L. Industrial Crops and Products, 51: 130-137.

Reddygunta, KKR., Beresford, R., Siller, L., Berlouis, L., and Ivaturi, A. 2023. Activated carbon utilization from corn derivatives for high-energy-density flexible supercapacitors. Energy & Fuels, 37(23): 19248-19265.

Rengaraj, S., Yeon, KH., Kang, SY., Lee, JU., Kim, KW., and Moon, SH. 2002. Studies on adsorptive removal of Co (II), Cr (III) and Ni (II) by IRN77 cation-exchange resin. Journal of hazardous materials, 92(2): 185-198.

Reti, W., Djoudi, W., Djinni, I., Saadaoui, B., Bensouici, F., and Chenchouni, H. 2024. Optimization of lead biosorption yield by Streptomyces humidus DBPb2 derived from a public waste dump using the response surface methodology. Water, Air, & Soil Pollution, 235(4): 489.

Revellame, ED., Fortela, DL., Sharp, W., Hernandez, R., and Zappi, ME. 2020. Adsorption kinetic modeling using pseudo-first order and pseudo-second order rate laws: A review. Cleaner Engineering and Technology, 1: 100032.

Robati, D. 2013. Pseudo-second-order kinetic equations for modeling adsorption systems for removal of lead ions using multi-walled carbon nanotube. Journal of nanostructure in Chemistry, 3: 1-6.

Said, TO., Al-Farhan, BS., El-Ghamdi, SA., and Awwad, N. 2024. Biosorbent treatment of fluorene using activated carbon derived from the pyrolysis process of date pit wastes. Scientific Reports, 14(1): 22039.

Sawant, N., Li, K., and Salam, A. 2022. Synthesis and Characterization of Corn Stover-Based Biosorbent with Superior Heavy Metal Absorption Properties. ACS Applied Engineering Materials, 1(1): 214-221.

Sekar, M., Sakthi, V., and Rengaraj, S. 2004. Kinetics and equilibrium adsorption study of lead (II) onto activated carbon prepared from coconut shell. Journal of colloid and interface science, 279(2): 307-313.

Shukla, A., Zhang, YH., Dubey, P., Margrave, JL., and Shukla, SS. 2002. The role of sawdust in the removal of unwanted materials from water. Journal of hazardous materials, 95(1-2): 137-152.

Sing, KSW., Everett, DH., Haul, RAW., Moscou, L., Pierotti, RA., Rouquérol, J., and Siemieniewska, T. 1985. Reporting physisorption data for gas/solid systems with special reference to the determination of surface area and porosity. Pure and Applied Chemistry, 57(4): 603–619.

Sun, CJ., Sun, LZ., and Sun, XX. 2013. Graphical evaluation of the favorability of adsorption processes by using conditional Langmuir constant. Industrial & Engineering Chemistry Research, 52(39): 14251-14260.

Sun, Y., Li, H., Li, G., Gao, B., Yue, Q., and Li, X. 2016. Characterization and ciprofloxacin adsorption properties of activated carbons prepared from biomass wastes by H3PO4 activation. Bioresource technology, 217: 239-244.

Sutirman, ZA., Sanagi, MM., Abd Karim, KJ., Ibrahim, WAW., and Jume, BH. 2018. Equilibrium, kinetic and mechanism studies of Cu (II) and Cd (II) ions adsorption by modified chitosan beads. International journal of biological macromolecules, 116: 255-263.

Tan, TL., Nakajima, H., and Rashid, SA. 2020. Adsorptive, kinetics and regeneration studies of fluoride removal from water using zirconium-based metal organic frameworks. RSC advances, 10(32): 18740-18752.

Tigori, MA., Atheba, P., and Trokourey, A. 2023. Production and Characterization of Green Biosorbent Based on Modified Corn Cob Decorated Magnetite Nanoparticles. Journal of Materials Science and Chemical Engineering, 11(2): 1-12.

Tseng, RL., and Wu, FC. 2009. Analyzing concurrent multi-stage adsorption process of activated carbon with a favorable parameter of Langmuir equation. Journal of the Taiwan Institute of Chemical Engineers, 40(2) 197-204.

Wang, S., Sun, Y., Fan, C., Wang, D., Liu, F., and Zhang, H. 2024. Enhanced biosorption of cadmium ions on immobilized surface-engineered yeast using cadmium-binding peptides. Frontiers in Microbiology, 15: 1496843.

Corresponding author's email address: aarasheed.cpe@buk.edu.ng

Wang, Z., Luo, P., Zha, X., Xu, C., Kang, S., Zhou, M., and Wang, Y. 2022. Overview assessment of risk evaluation and treatment technologies for heavy metal pollution of water and soil. Journal of Cleaner Production, 379: 134043.

Zafar, S., Fatima, S., Asad, F., Nazir, MM., Batool, S., and Ashraf, A. 2024. Combating Lead (Pb) Contamination: Integrating Biomonitoring, Advanced Detection, and Remediation for Environmental and Public Health. Water, Air, & Soil Pollution, 236(1): 8.

Zhang, Y., Zheng, R., Zhao, J., Zhang, Y., Wong, P. K., and Ma, F. 2013. Biosorption of zinc from aqueous solution using chemically treated rice husk. BioMed research international, 1: 365163.

Corresponding author's email address: aarasheed.cpe@buk.edu.ng